

# Quantum Tunneling via Finite Element

Jerome Troy

May 13, 2021

## 1 Introduction

In this paper, we examine tunnelling solutions to the fundamental equation in quantum mechanics: the Schrödinger equation for quantum particles which only interact with an external potential (and not with each other).

$$i\hbar \frac{\partial \Psi}{\partial t} = -\frac{\hbar^2}{2m} \nabla^2 \Psi + V\Psi \quad (1)$$

Here  $\Psi = \Psi(\mathbf{x})$  is the wave function describing a quantum mechanical particle,  $t$  is time,  $V = V(\mathbf{x}, t)$  is the potential with which the particle interacts. The constant  $m$  is the mass of the particle, and  $\hbar$  is Planck's constant divided by  $2\pi$  [3].

We consider the following scenario. A particle is confined to a well in  $\mathbb{R}^2$ . It passes by a ring-shaped well which is connected to a second well leaving the system (see figure 1). Such a situation is the problem of interest in characterizing quantum ring resonators [2, 5, 6].

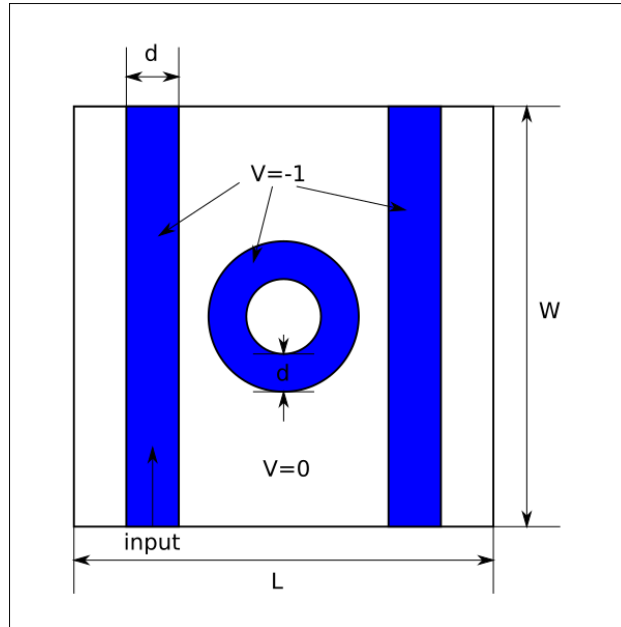


Figure 1: Sketch of Ring resonator. The domain excluding the shaded regions is  $\Omega_0$ . The two shaded rectangles are  $\Omega_1$  and  $\Omega_2$  from left to right. Finally the center ring is  $\Omega_3$ . The entire domain is  $\Omega = \Omega_0 \cup \Omega_1 \cup \Omega_2 \cup \Omega_3$ .

The question we will answer is the following. At steady state (or the long time limit), what is the probability the wave will tunnel through the ring, and to the other tube on the right side of the domain? We will solve this problem using finite elements, and using the Python library FEniCS, which will take care of the heavy lifting in constructing the finite element representation.

Let  $\Omega_0$  be the region without color, a rectangle of width  $W$  and length  $L$ , excluding the colored regions. The two long rectangles, in order from left to right are  $\Omega_1$  (the input tube) and  $\Omega_2$  (the output tube) respectively. Finally, the ring in the center is  $\Omega_3$  (this is the ring resonator). The domain boundary is broken up as follows. The input boundary,  $\Gamma_{\text{in}}$  is the bottom of the left tube, labeled input. Here  $\Psi$  is specified via a Dirichlet condition. On the other 3 blue boundaries, which we will call  $\Gamma_{\text{out}}$ , we enforce an open boundary and allow the wave to leave the system. This is done through

$$\frac{\partial \Psi}{\partial t} - i \frac{\hbar}{m} \frac{\partial \Psi}{\partial n} = 0 \quad x \in \Gamma_{\text{out}}.$$

Finally, on all uncolored boundaries, denoted  $\Gamma_D$ , a zero-Dirichlet condition is enforced.

## 1.1 Nondimensionalization

Nondimensionalizing the problem is essential since  $\hbar \approx 10^{-34} J \cdot s$  in S.I. units. Let the spacial scaling be  $d$ , the width of each of the long potential wells. This induces a time scaling of  $\frac{2md^2}{\hbar}$ . Finally there is an energy scaling of  $V_0$ , which characterizes the strength of the potential. To summarize, if  $\tilde{\mathbf{x}}, \tilde{t}, \tilde{V}$  all have units, then

$$\tilde{\mathbf{x}} = d \cdot \mathbf{x}, \quad \tilde{t} = \frac{2md^2}{\hbar} t, \quad \tilde{V}(\tilde{\mathbf{x}}) = V_0 V(\mathbf{x}). \quad (2)$$

Let  $\nu = \frac{2md^2 V_0}{\hbar^2}$ . The nondimensionalized problem then reads

$$i \frac{\partial \Psi}{\partial t} = -\nabla^2 \Psi + \nu V(\mathbf{x}) \Psi. \quad (3)$$

Here, the form of  $V(\mathbf{x})$  is

$$V(\mathbf{x}) = \begin{cases} -1 & \mathbf{x} \in \Omega_1 \cup \Omega_2 \cup \Omega_3 \\ 0 & \mathbf{x} \in \Omega_0 \end{cases}. \quad (4)$$

## 1.2 Boundary and Initial Conditions

An input is specified on the lower portion of the left-most shaded rectangle. This will be denoted by the region  $\Gamma_{\text{in}}$ . All other boundaries of  $\Omega$  which are also boundaries of  $\Omega_i$  for  $i = 1, 2$  will be denoted  $\Gamma_{\text{out}}$ . Finally, the rest of the boundary will be denoted  $\Gamma_D$ .

On  $\Gamma_{\text{in}}$ , there is a specified Dirichlet boundary condition:  $f(\mathbf{x}, t)$ , and on  $\Gamma_D$  the Dirichlet condition is zero. Lastly, on  $\Gamma_{\text{out}}$  we specify an outflow boundary condition. In quantum mechanics, the momentum operator, in this dimensionless system:  $\hat{\mathbf{p}} = -i\nabla$ . The outflow condition relates  $\partial_t \psi$  with the momentum. All together the boundary conditions are

$$\text{Boundary Conditions} = \begin{cases} \Psi(\mathbf{x}, t) = 0 & \mathbf{x} \in \Gamma_D \\ \Psi(\mathbf{x}, t) = f(\mathbf{x}, t) & \mathbf{x} \in \Gamma_{\text{in}} \\ \frac{\partial \Psi}{\partial t} = i \frac{\partial \Psi}{\partial n} & \mathbf{x} \in \Gamma_{\text{out}} \end{cases} \quad (5)$$

Where  $f(\mathbf{x}, t)$  is a prespecified function.

Finally for simplicity, we take an initial condition of an empty system: i.e.

$$\Psi(\mathbf{x}, 0) = 0.$$

## 2 Constructing the Weak Formulation

Since FEniCS will be doing the heavy lifting for the matrix construction and equation solving, the weak formulation will be optimized to fit this framework. FEniCS does not support complex numbers. To deal with this, we will use FEniCS to build the matrix formulation of the problem, then deal with an ODE solver which can handle complex numbers.

In sticking with the quantum mechanical theme, I will be using bra-ket notation (little bit late for Halloween, but okay). That is  $\Psi$  will be known as  $|\Psi\rangle$ . The term inside the ket:  $|\cdot\rangle$  can be anything, as it is a label. For now we will leave it as  $|\Psi\rangle$ . The bar and angle denote that  $\Psi$  is an element of the Hilbert space  $\mathcal{V}$ . Next I will denote the linear functional by a bra:

$$\langle\Phi|\cdot = \int_{\Omega} \Phi^* \cdot dx.$$

That is  $\langle\Phi|$  is the linear functional built by the  $L^2$  inner product with  $|\Phi\rangle$ . Again, what is inside the  $\langle\cdot|$  is simply a label, and for now it will be left as  $\langle\Phi|$ . Finally an inner product with an operator  $\mathcal{O}$  will be denoted:

$$\langle\Phi|\mathcal{O}|\Psi\rangle = \int_{\Omega} \Phi^* \mathcal{O}[\Psi] dx.$$

On the interior of the domain, the Schrödinger equation can now be written in variational form:

$$i \langle\Phi|\partial_t|\Psi\rangle = \langle\Phi|-\nabla^2|\Psi\rangle + \langle\Phi|V|\Psi\rangle.$$

At this point, we can integrate the laplacian term by parts:

$$\begin{aligned} \langle\Phi|-\nabla^2|\Psi\rangle &= - \int_{\Omega} \Phi^* \nabla^2 \Psi dx \\ &= - \int_{\partial\Omega} \Phi^* \frac{\partial\Psi}{\partial n} d\sigma + \int_{\Omega} \nabla\Phi^* \cdot \nabla\Psi dx. \\ &= - \int_{\partial\Omega} \Phi^* \frac{\partial\Psi}{\partial n} d\sigma + \langle\nabla\Phi|\nabla\Psi\rangle \end{aligned}$$

For  $\mathcal{V}$  we choose the subspace of  $H^1(\Omega)$  which is zero on both  $\Gamma_D$  and  $\Gamma_{in}$ . This term then becomes

$$\langle\Phi|-\nabla^2|\Psi\rangle = - \int_{\Gamma_{out}} \Phi^* \frac{\partial\Psi}{\partial n} d\sigma + \langle\nabla\Phi|\nabla\Psi\rangle.$$

Next, on  $\Gamma_{out}$ , the boundary condition was chosen such that

$$\frac{\partial\Psi}{\partial t} = i \frac{\partial\Psi}{\partial n} \implies \int_{\Gamma_{out}} \Phi^* \frac{\partial\Psi}{\partial n} d\sigma = -i \int_{\Gamma_{out}} \Phi^* \frac{\partial\Psi}{\partial t} d\sigma.$$

Therefore the Schrödinger equation now reads

$$i \langle\Phi|\partial_t|\Psi\rangle = \langle\nabla\Phi|\nabla\Psi\rangle + \langle\Phi|V|\Psi\rangle + i \int_{\Gamma_{out}} \Phi^* \frac{\partial\Psi}{\partial t} d\sigma.$$

At this point, we can make a finite dimensional approximation. FEniCS will generate a triangulation,  $\mathcal{T}_h$  for  $\Omega$ . Using standard  $C^0 - P^1$  elements, we get a Lagrange basis for our finite dimensional subspace of  $\mathcal{V}$ . It should be noted we are taking  $\mathcal{V}$  to be a real space, the complex parts of the wave functions will be incorporated into the time variation. Let this basis for  $\mathcal{V}$  be denoted by  $\phi_j$  for  $j = 0, 1, \dots, N$ . We then make the ansatz

$$\Psi(x, t) = \sum_j \alpha_j(t) \phi_j(x).$$

Here  $\alpha_j : \mathbb{R}_+ \rightarrow \mathbb{C}$  are complex functions, and  $\phi_j$  are real. The Schrödinger equation reads in variational form

$$i \sum_{\ell} \underbrace{\langle\phi_k|\phi_{\ell}\rangle}_{M_{k\ell}} \alpha'_{\ell} = \sum_{\ell} \left( \underbrace{\langle\nabla\phi_k|\nabla\phi_{\ell}\rangle}_{S_{k\ell}} + \underbrace{\langle\phi_k|V|\phi_{\ell}\rangle}_{V_{k\ell}} \right) \alpha_{\ell} + i \sum_{\ell} \alpha'_{\ell} \underbrace{\int_{\Gamma_{out}} \phi_k \phi_{\ell} d\sigma}_{B_{k\ell}}.$$

Where  $M$  is the mass matrix,  $S$  the stiffness matrix,  $V$  is a “potential” matrix, and  $B$  is a “boundary” matrix. In matrix form this reads

$$i(M - B)\alpha' = (S + V)\alpha.$$

Here  $M, B, S, V$  are all real matrices, and  $\alpha$  are complex vectors.

Once the matrices are assembled, time stepping is done using the Crank-Nicolson method. This reads to solving

$$\left[ i(M - B) - \frac{\Delta t}{2}(S + V) \right] \alpha^{n+1} = \left[ i(M - B) + \frac{\Delta t}{2}(S + V) \right] \alpha^n.$$

For  $\alpha^{n+1}$  where  $\alpha^n = \alpha(n\Delta t)$  is assumed to be given. The initial condition:  $\Psi \equiv 0$  translates to  $\alpha^0 = 0$ .

It should be noted that to account for the input boundary condition, we can index the matrices using  $I_D$  for the nodes on  $\Gamma_D$  and  $I_{in}$  for the nodes on  $\Gamma_{in}$ . Since on  $\Gamma_D$ ,  $\Psi = 0$  this does not contribute. However we can extract the free indices (those not in  $I_D$  or  $I_{in}$ ) and extract those on  $I_{in}$ . Then the problem reads as:

$$\begin{aligned} \left[ i(M - B) - \frac{\Delta t}{2}(S + V) \right]_{\text{free}} \alpha_{\text{free}}^{n+1} &= \left[ i(M - B) + \frac{\Delta t}{2}(S + V) \right]_{\text{free}+in} \alpha_{\text{free}+in}^n \\ &\quad - \left[ i(M - B) + \frac{\Delta t}{2}(S + V) \right]_{in} f(x \in \Gamma_{in}, t^{n+1}). \end{aligned}$$

### 3 Results and Discussion

We tested the solution scheme using a quasi-uniform mesh with the minimum cell diameter:  $h_{\min} = 0.1$ . The time stepping used a maximum time of 5 with 5000 time steps. Below are several figures describing the time evolution of the problem. Each figure has the probability density function (pdf) plotted, where the pdf is given by

$$\rho(x, t) = \Psi^*(x, t)\Psi(x, t) = \sum_j |\alpha_j(t)|^2 \phi_j^2(x).$$

Which is pointwise multiplication. It should be noted that what is computed is not a pdf, since its integral may not be 1. However taking ratios of integrals will give the relative probabilities of the particle existing in specified regions [7]. Further, the pdf is plotted using a log scale, to better see regions of low probability.

The results show that the wave carries its momentum through the system, and initially behaves as if it were a car going around a turn. However after time  $t = 1.5$ , the system equilibrates, and the wave function no longer appears to exhibit a preferential traversal direction. These figures can be seen in the appendix.

Next consider the transmission coefficient. This is given by the output amplitude divided by the input amplitude. Here we compute this via the following ratio

$$C_{\text{trans}} = \frac{\langle \Psi | \mathbb{1}_{\Omega_0} | \Psi \rangle}{\langle \Psi | \mathbb{1}_{\Omega_1} | \Psi \rangle} = \left( \int_{\Omega_1} \rho(x, t) dx \right)^{-1} \int_{\Omega_0} \rho(x, t) dx. \quad (6)$$

This quantity is variable with time. This can be seen in figure 8. Here the transmission coefficient can be seen to peak at just below 4%. Furthermore it can be seen transmission starts to occur after time  $t = 1$ . It should be noted that the eigenvalues of the Schrödinger equation are all purely imaginary, which lie on the boundary of the stability region of the time stepping method - Crank-Nicolson. As a result, it is not surprising to see some high oscillation modes in the transmission coefficient.

### 4 Conclusions

As a proof-of-concept experiment, we were able to deduce the transmission of a quantum mechanical particle through a ring resonator using finite elements.

Future improvements could include testing various geometries or input conditions, as well as improving the nonreflecting condition on the output boundaries. According to [1], an optimal non-reflecting boundary will involve implementing a fractional time derivative on the boundary.

## References

- [1] A. ARNOLD, *Open boundary conditions for wave propagation problems on unbounded domains*. 2007.
- [2] S. T. FARD, S. M. GRIST, V. DONZELLA, S. A. SCHMIDT, J. FLUECKIGER, X. WANG, W. SHI, A. MILLSPAUGH, M. WEBB, D. M. RATNER, K. C. CHEUNG, AND L. CHROSTOWSKI, *Label-free silicon photonic biosensors for use in clinical diagnostics*, International Society for Optical Engineering, (2013).
- [3] D. J. GRIFFITHS, *Introduction to Quantum Mechanics*, Pearson Education, Inc., New Jersey, 2005.
- [4] A. LOGG, K.-A. MARDAL, G. N. WELLS, ET AL., *Automated Solution of Differential Equations by the Finite Element Method*, Springer, 2012.
- [5] T.-B. WANG, X.-W. WEN, C.-P. YIN, AND H.-Z. WANG, *The transmission characteristics of surface plasmon polaritons in ring resonator*, The Optical Society, (2009).
- [6] A. L. WASHURN, L. C. GUNN, AND R. C. BAILEY, *Label-free quantitation of a cancer biomarker in complex media using silicon photonic microring resonators*, Analytical Chemistry, (2009).
- [7] L. WASSERMAN, *All of Statistics: A Concise Course in Statistical Inference*, Springer, New York, 2005.

## A Figures for Results

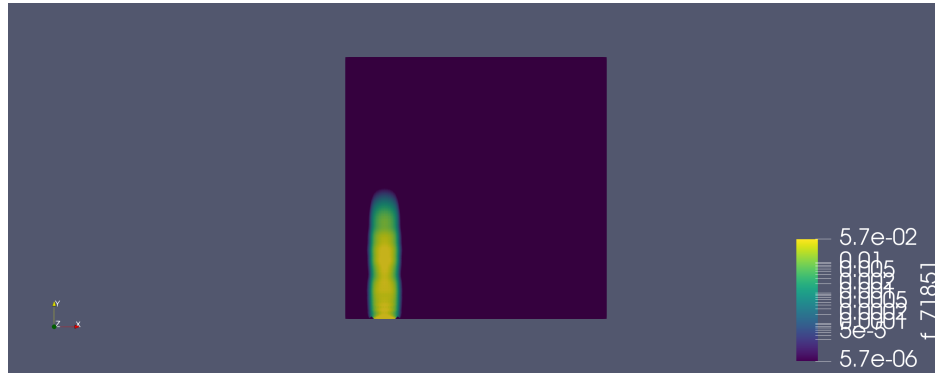


Figure 2: Entrance profile of the wave into the input tube, taken at  $t = 0.2$ . The wave has entered the input tube but has yet to enter the ring resonator

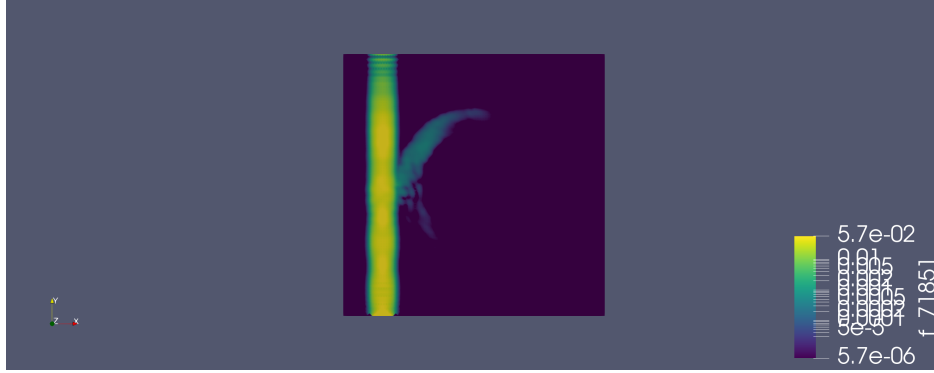


Figure 3: At this point, the wave has spilled over into the ring resonator, taken at  $t = 0.4$ . Note that the momentum of the wave (towards the positive  $y$  direction) causes it to fill the top part of the ring first.

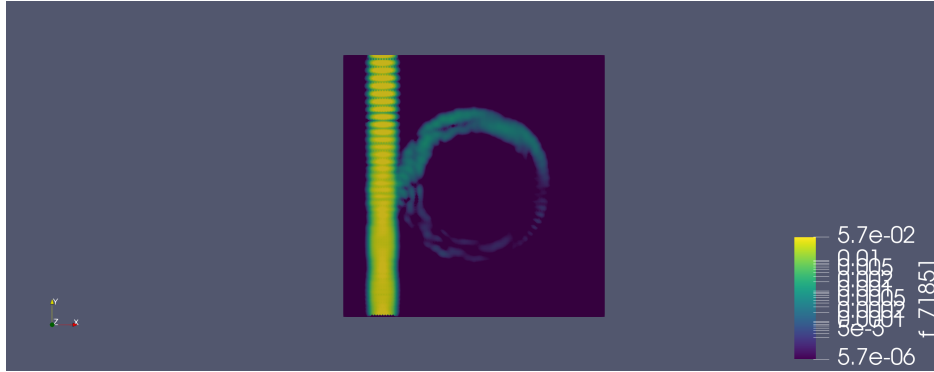


Figure 4: The wave covers nearly all the ring at this point, albeit at a much lower intensity than at the input. This occurs at  $t = 0.6$ .

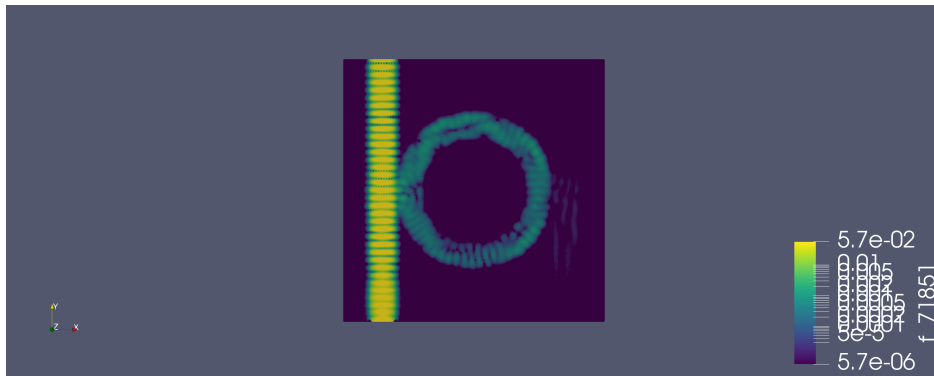


Figure 5: Once the wave fills the ring nearly uniformly, the wave begins to spill over into the exit tube. This snapshot was taken at time  $t = 0.8$ .

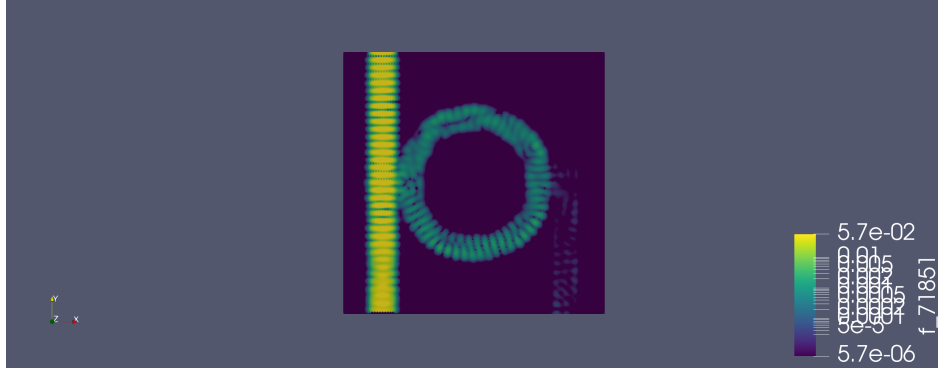


Figure 6: At time  $t = 1$  the wave reaches the exit point of the output tube. It's initial preference is having flipped  $180^\circ$  and returning to the direction it entered.

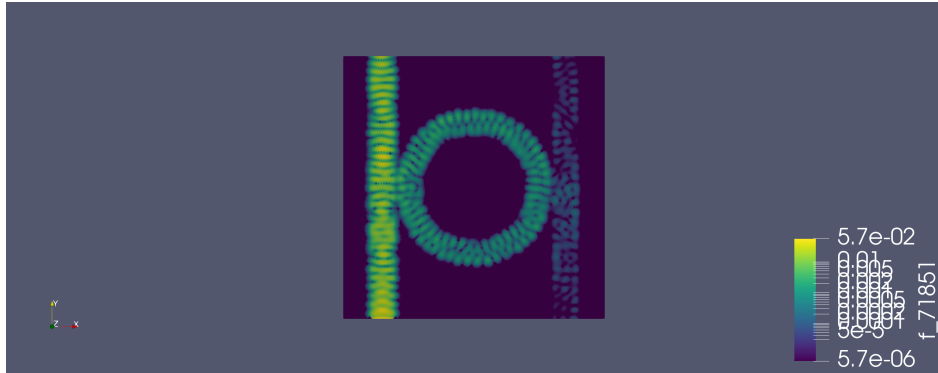


Figure 7: By time  $t = 1.5$  the wave has come to a relatively stable state, and has filled the exit tube. It no longer appears to exlude a preference for exiting out the top or bottom.

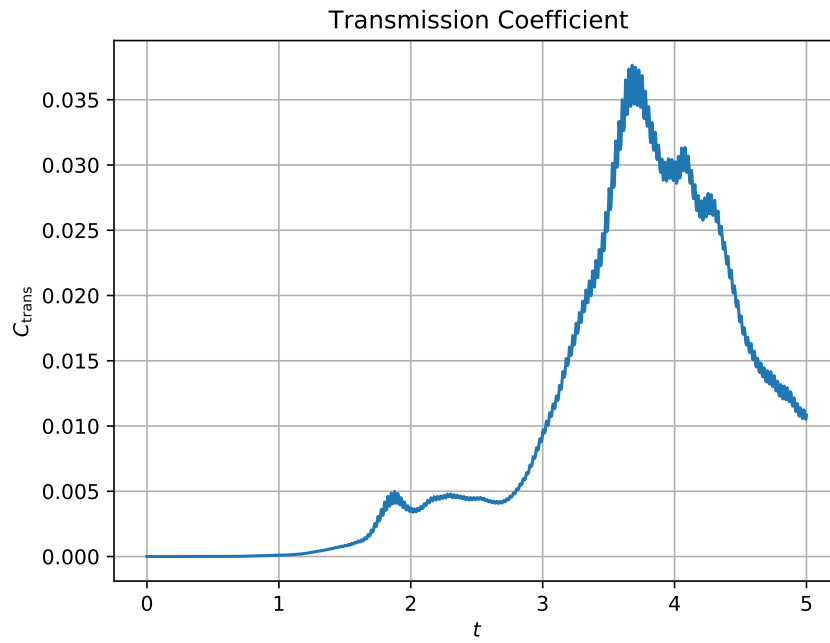


Figure 8: Time variation of transmission coefficient. It can be seen the transmission peaks after  $t = 3.5$  then dips back down. It can also be seen that no more than 4% of the wave is ever transmitted through to the output tube.